JOURNAL OF THE BALKAN GEOPHYSICAL SOCIETY, Vol. 5, No 3, August 2002, p. 97-106, 15 figs.

The use of geophysical prospecting for imaging the aquifer of Lakka carbonates, Mandoudi Euboea, Greece

Ioannis F. Louis[1], Antonios P. Vafidis[2], Filippos I. Louis[1] and Nikolaos Tassopoulos[2]

[1] Geophysics-Geothermy Division, Geology Department, University of Athens, Panepistimiopolis Ilissia, Athens, 15784 Greece.
[2] Applied Geophysics Laboratory, Department of Mineral Resources Engineering, Technical University of Crete, Chania, Greece.

(Received 20 March 2001; accepted 20 January 2002)

Abstract: *Non-destructive seismic reflection and resistivity imaging techniques have been successfully applied at Mandoudi, Euboea aiming to contribute with essential information for the simulation of the Lakka karst aquifer. A seismic reflection and refraction survey was carried out to determine the active thickness of the karst aquifer. Electrical tomography indicated that there is no hydraulic communication between Lakka aquifer and the Nileas River. The resulting geophysical models were useful for building a conceptual geological/hydrogeological model of the aquifer. This model also contributed by guiding a drilling program for the irrigation of the plain area in the north and east of Mandoudi.*

Key Words*: Aquifer Simulation, Seismic Methods, Resistivity Imaging.*

INTRODUCTION

In the context of investigating the hydrogeological conditions of the area north of Mandoudi, Euboea, the Geophysics and Applied Geology Divisions, University of Athens conducted an exploration project in 1998. Amongst other objectives, providing information about the water balance in the Lakka carbonates located north of Mandoudi was also the subject of this project (Fig. 1).

The construction of the irrigation network for the plain area north and east of Mandoudi greatly depends on the estimation of water balance in the Lakka carbonates. For the assessment of the water balance, the knowledge of all kinds of water contribution as well as the water capacity of the carbonates is essential. Note that six boreholes with important water supply (Fig. 2) have been drilled in this karst aquifer. However, the limited outcropping area of the carbonates does not justify the apparently great potential of the Lakka karst system. Therefore, geophysical images of the subsurface are necessary to verify hydraulic communication between the geological formations.

Hydraulic parameter estimation and assessment of Lakka aquifer are based on simulation of the aquifer system. The thickness of the karst aquifer is a key parameter for the simulation. It was not possible; however, to determine the thickness from the drilling program, since the boreholes in Lakka did not reach the impermeable formation that underlies the aquifer.

Another key point is whether Nileas River, which crosses Lakka limestones, enriches this aquifer. During pumping tests for boreholes Γ0 and Γ1 (Fig. 1) no infiltration of waters from the river towards the Lakka system was observed. This indicates that the river does not enrich the aquifer. Clay deposits at the channel's base may act as a waterproof bed. A geophysical survey was conducted to investigate the existence of an aquitard at the channel's base and to estimate the active thickness of the karst aquifer.

GEOLOGY AND HYDROGEOLOGY

In the study area, a series of formations of the Subpelagonic – Pelagonic zone (Lekkas and Alexopoulos, 1998), consisting of limestones, dolomites, mélanges and peridotites, is covered by a series of Neogene and Quaternary deposits. The hydrogeological regime in the wider area of study is related to the lithostratigraphy and the tectonic structure of the geological formations. The Lakka carbonates that are outcropping north of Mandoudi, exhibit hydrogeologic interest (Fig. 1). The intensely fractured limestones and ophiolites located south of Mandoudi supply with water the Lakka aquifer (Fig. 3). The carboniferous mass of Lakka is thrusted on the mélange formation that acts as a barrier. Thus, water cannot be discharged to the Aegean Sea.

SEISMIC SURVEY FOR THE DETERMINATION OF THE ACTIVE AQUIFER THICKNESS

The seismic survey was carried out along two profiles (Fig. 1) that are spaced 20 m apart in the east–west di-

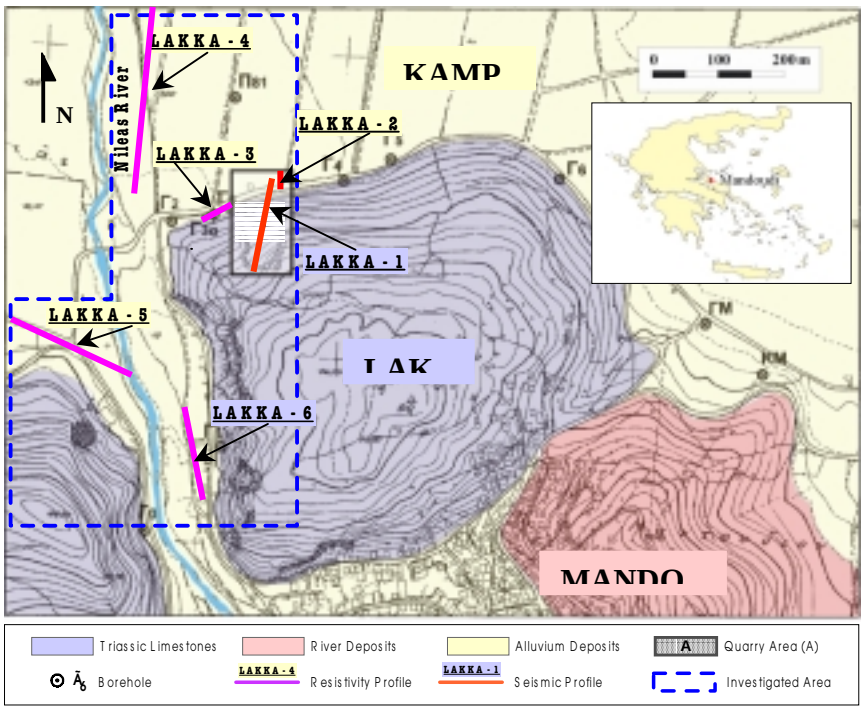

FIG. 1. Location and geologic map of the survey area.

FIG. 2. Pumping test in borehole Γ2.

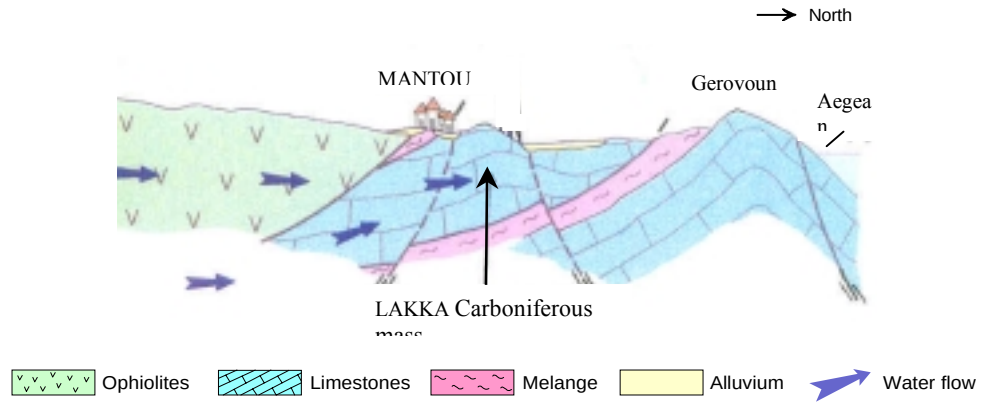

FIG. 3. Schematic geologic section of the area under investigation.

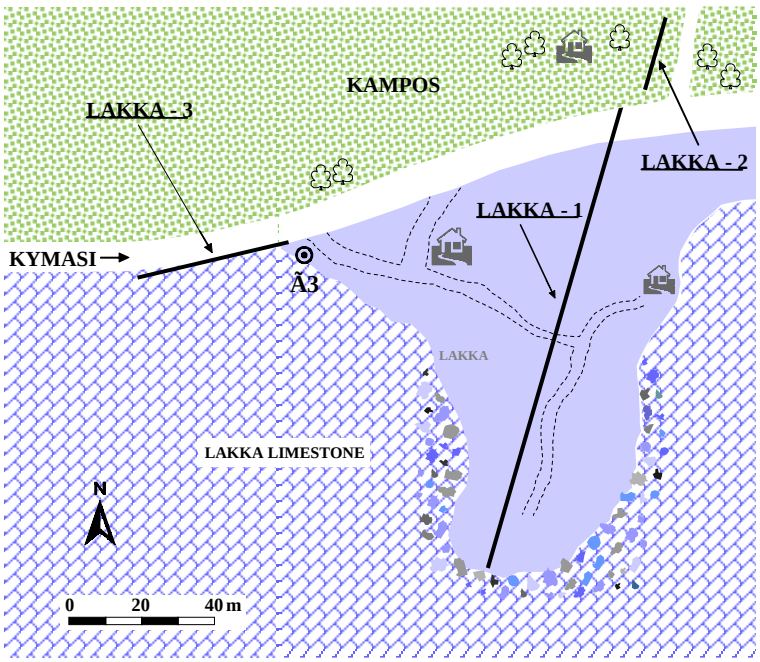

FIG. 4. Map of Lakka quarry with the location of the geophysical lines.

FIG. 5. Survey area with the location of the seismic reflection line LAKKA-1.

rection (Louis, 1998). A walk-away noise test was initially performed along "LAKKA -1" line. Subsequently, the roll along technique was applied in order to collect multifold data. The seismic refraction experiment was conducted along the "LAKKA -2" line. The recording assembly consisted of 14 Hz vertical component geophones connected to a 24-channel seismograph (EG&G Geometrics ES2401).

The noise test is necessary for the design of the seismic reflection experiment. During the walk-away test, the geophone array has been progressively moved away from the shot point. Using the seismic records obtained from this test identified the ground rolls as well as the reflections. The optimum source-receiver offset was then selected for the near and far geophones.

Data Acquisition

Since the terrain of the outcropping limestones in Lakka is quite steep (Figs. 1 and 5), the seismic reflection survey was conducted in an abandoned quarry (Figs 4 and 5). The geophone spacing and the minimum source to receiver offset were set to 1.5 m and 5 m, respectively, for the noise test. The presence of the airwaves and ground roll was strong on the seismic records. However, they didn't cause any serious problem since the reflections were identified without any difficulty. In order to record clear reflections from the target horizons, the optimum geophone spacing for the seismic reflection experiment was selected as 2.5 m and the minimum source-receiver offset, as 30 m.

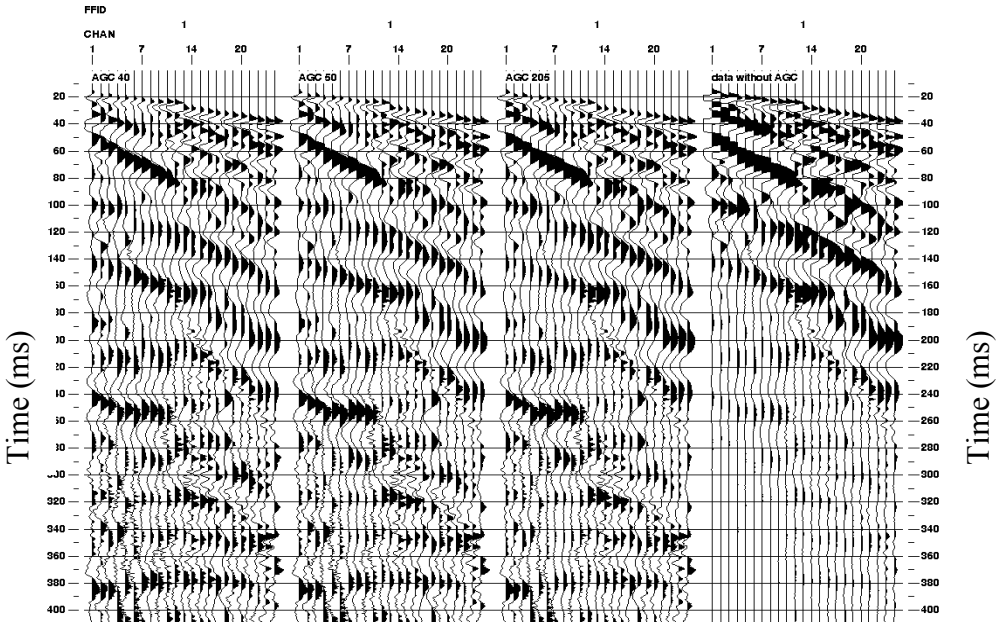

FIG. 6. Parameter test for the determination of the optimum AGC window.

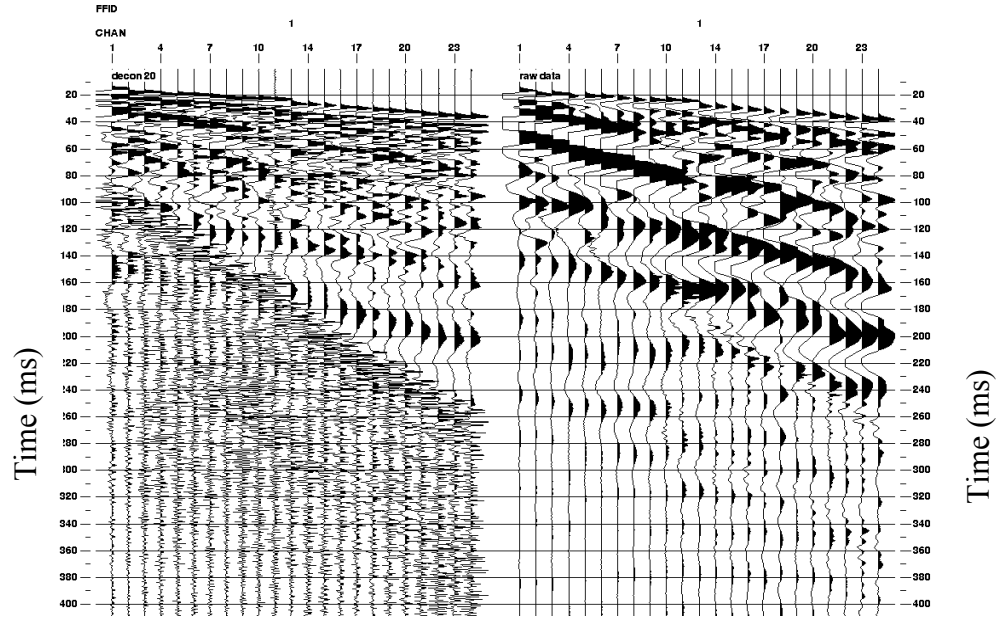

FIG. 7. Comparison of raw (right) and filtered (left) data with a minimum phase deconvolution operator.

For the seismic reflection experiment the depth of the shot holes, dug with a hand auger, was 0.5 m and the shot spacing, 2.5 m. The geophones and the shot formed an offend array. For unacceptable quality records, the source was recharged. For shots located at horizontal distances less than 57.5 m, the number of active channels was 24. The active channels were consequently reduced becoming 13 for the last shot corresponding to 80 m distance. The total length of the reflection profile was 140 m, the maximum fold, 12 and the CMP spacing, 1.25 m. The acquisition parameters and equipment are given in Table I.

Table 1. Survey parameters and equipment.

Recorder	ES-2401Geometrics 24 channels
Energy source	Dynamite charges (100gr)
Receivers	Vertical (14Hz) Mark products
Shot spacing	2.5m
Receiver spacing	2.5m
Offset Min/Max	30/140m
Maximum fold	12
Record length	409 ms
Time sampling interval	1ms
Section length	140 m
Shot-receiver geometry	Offend

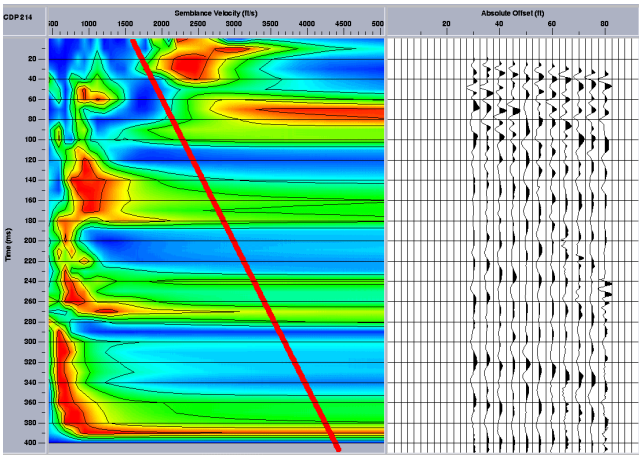

FIG. 8. Velocity analysis with the semblance.

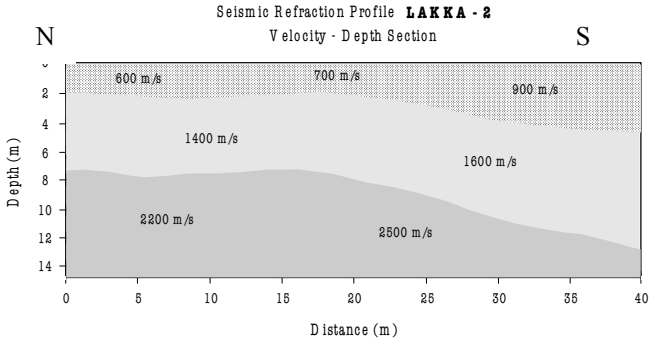

FIG. 9. Velocity-depth section for the refraction line LAKKA-2.

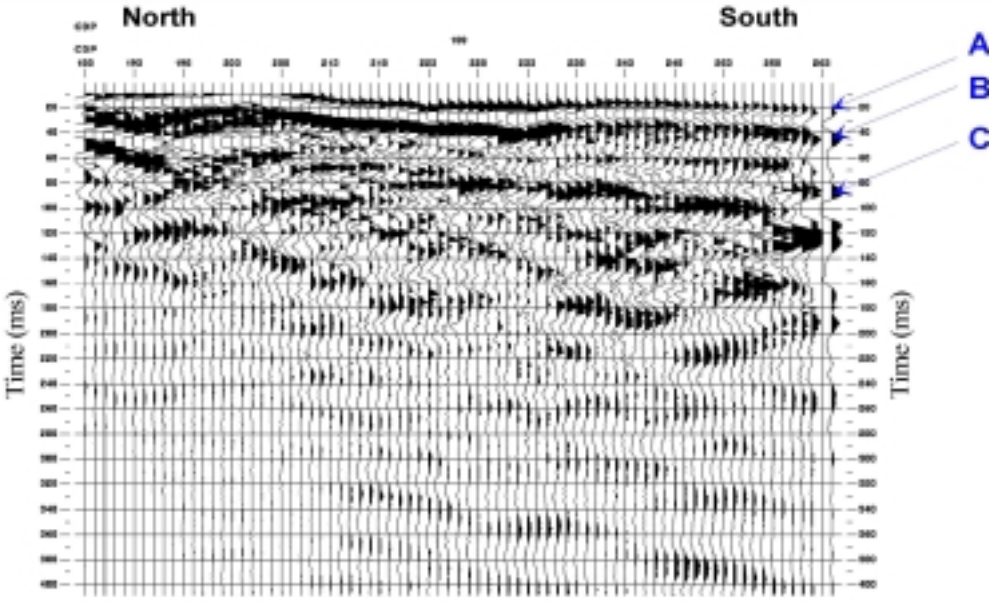

FIG. 10. CMP stacked section.

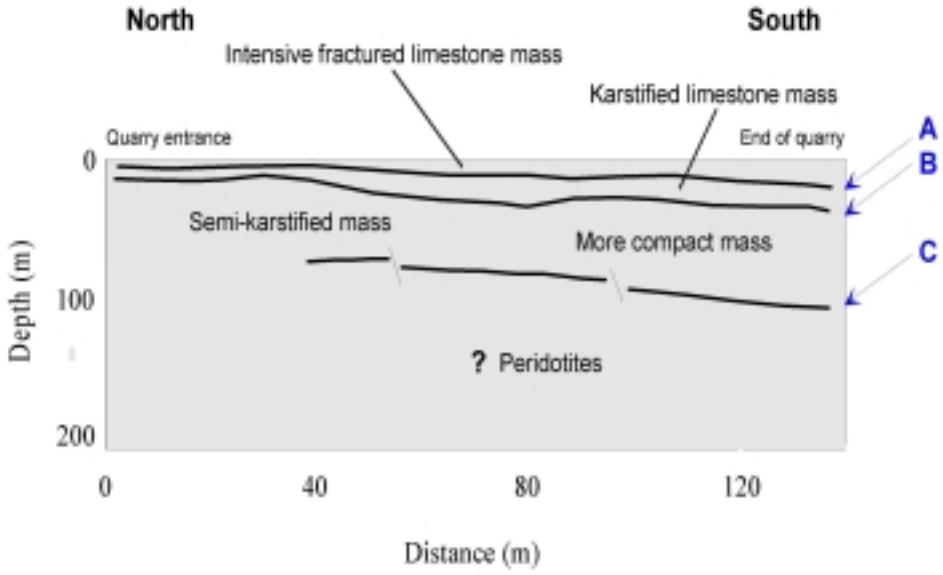

FIG. 11. Interpretation of the reflection profile.

Data Processing

Seismic data were processed at the Applied Geophysics Laboratory, Department of Mineral Resources Engineering, Technical University of Crete, on a SUN workstation using the commercial software package ProMAX. Noise attenuation filtering was not applied, because a first examination of raw seismic records showed well-separated reflected events at two-way time of 20-60 ms.

Although surgical mute is a routine step in data processing, it proved to be extremely difficult to mute out refracted events without destroying or seriously damaging shallow reflections. Automatic gain control (AGC) enhanced the low amplitude reflected waves. The gain was calculated by setting the AGC time window to 205 ms and taking the mean of the samples in this window. The optimum window length was selected from the comparison of AGC filtered data corresponding to the time window of 40 ms, 50 ms and 205 ms (Fig. 6).

The processing steps are presented in Table 2. A spiking deconvolution operator was applied to suppress the waveform of the seismic source. The operator's length was determined from the autocorrelation of the seismograms corresponding to several shots. Reflections arriving at times greater than 100 ms are clearly shown on the filtered shot gather (Fig. 7). Next f-k filtering was performed. Velocity analysis was carried out using the semblance (Fig. 8).

Table 2. Data processing flow.

Data reformat (SEG-2→SEG-Y)
Geometry and trace editing
Trace kill/Reverse
Automatic Gain Control (AGC) scaling
Minimum phase spiking deconvolution
Frequency-Wave number f-k analysis filtering
Sorting to CMP gathers
Velocity analysis/manipulation
NMO correction (Stretch mute 30%)
Stack

The dominant frequency for the reflected waves is 125 Hz. The radius of the first Fresnel zone for the shallowest P-wave reflector appearing at two-way time 35 ms is 9 m. Since the CMP subsurface sampling was 1.25 m, there are at least 7 points per Fresnel zone. Therefore, the reflector sampling is reasonable. The vertical resolution can be estimated using the 1/8 wavelength criterion (Widess, 1978). For an average P-wave velocity of 1500 m/s, the dominant wavelength is 13 m, which in turn gives a vertical resolution of 1.6 m.

The seismic velocities for the very shallow geological formations were estimated from a high-resolution seismic refraction survey conducted near the reflection line. The seismic source was a sledgehammer and the geophone spacing was 2 m. The velocity-depth section (Fig. 9), deduced from the generalized reciprocal method (Palmer, 1981), and corresponds to depths less than 15 m. The dynamic (NMO) correction was applied using a stretch factor of 30%. Next, the NMO corrected common-midpoint gather traces are summed in order to obtain the stacked section (Fig. 10).

Interpretation of the Reflection Profile

On the stacked section (Fig. 10) three almost horizontal reflectors can be traced along the line down to 130 ms (about 100 m depth). The signal to noise ratio becomes fairly low for two-way times greater than 90 ms, though reflection energy is still evident. The reflector A with mean depth of 9 m (Figs. 10 and 11) is interpreted as the base of an intensively fractured limestone zone. According to the refraction depth section the seismic velocity of this layer ranges from 1400 to 1600 m/s (Fig. 9). The depth of the refractor at the base of the intensively fractured limestone layer varies from 7 to 12 m on this section. The 2 m depth deviation between the reflector A and the shallow refractor may originate from elevation differences between the seismic lines "LAKKA -1" and "LAKKA -2".

The seismic refraction depth section also shows a very shallow refractor at depth of about 3 m (Fig. 9). This refractor according to information from the nearby monitoring borehole Γ3 corresponds to the water table. The water table is also present on the resistivity tomography image along the line LAKKA-3, (Fig. 12) which is located west of borehole Γ3 (Fig. 4). On the resistivity image the broken line indicates the water table, located at 7m depths near the borehole Γ3. The stacked section "LAKKA-1", however, does not show the water table reflection. The absence of the water table reflection is attributed to the difficulty in imaging very shallow reflectors.

A second reflector B (Figs 10 and 11) is imaged at 30 ms (25 m depth). The mean depth to the reflector B is 17 m. This reflector is attributed to the base of karstified limestone based on the information available from the lithology section of the nearby borehole Γ3, (Fig. 11). The interval velocity of this layer ranges from 2200 to 2400 m/s. The velocity variation of this layer is similar to the one of the third layer on the refraction depth section (Fig. 9). Low amplitudes of reflection event B at CDPs 238 to 260 may be due to increasing karstification.

Finally, the third reflector C (Figs 10 and 11) at two-way time 80-120 ms (or depth 100 m) is attributed to the limestone basement. The lateral interval velocity variation (2600 to 3000 m/s) of the limestone layer (Fig. 11) was interpreted as the transition from a semi-karstified limestone, corresponding to the quarry entrance, to a more compact mass toward the south end of the quarry.

DETERMINATION OF THE RIVER'S BASE STRUCTURE BY ELECTRICAL TOMOGRAPHY

To meet the next objective of the geophysical investigation namely, whether Nileas River enriches the karst aquifer of Lakka mass, a resistivity tomography survey was conducted in the wider area of Lakka mass. In particular, the purpose of this survey was to clarify if there was an aquitard on the river's base. Four resistivity profiles were conducted parallel and perpendicular to the river (Fig. 1).

In resistivity studies, a low-frequency current is introduced in the ground and the potential difference between two electrodes, provides information about the resistivity of the subsurface (Telford *et al*., 1990). The number and the configuration of electrodes can vary and the apparent resistivity measurement depends not only on the ratio of the potential difference and current amplitude but also on the geometry of the electrode configuration. In electrical tomography, a multielectrode array is deployed and using pairs of current and potential electrodes makes a large number of successive measurements. The apparent resistivity measurements are then inverted to obtain a two-dimensional (2D) resistivity image.

Data Acquisition and Processing

Four lines namely, LAKKA-3, LAKKA-4, LAKKA-5 and LAKKA-6 (Fig. 1) were scanned using the electrical tomography method by the help of the Wenner-Schlumberger array with a maximum *n* separation (ratio of maximum and minimum electrode spacing) equal to 9. The data were collected with the SYSCAL R1 Plus resistivity meter (IRIS). The survey lines were located along existing roads and paths avoiding physical obstacles like buildings and fences. The minimum electrode spacing was set to 20 or 50 m.

The apparent resistivity pseudosection produces a distorted image of the subsurface resistivity. Inversion of the field observations is the standard procedure to obtain an estimate of the true resistivity distribution. In this work, a smoothness-constrained algorithm was used to invert the apparent resistivity data (Tsourlos, 1995; Tsourlos *et al*., 1998). The algorithm is iterative and fully automated. A reliable 2.5-D finite-element method is used for the calculation of the Jacobean matrix and the apparent resistivity. The inversion estimates a resistivity model by minimizing the difference between the observed and the calculated data. The roughness of the resistivity model is also minimised in the smoothness constrained inversion method by imposing a smoothness condition.

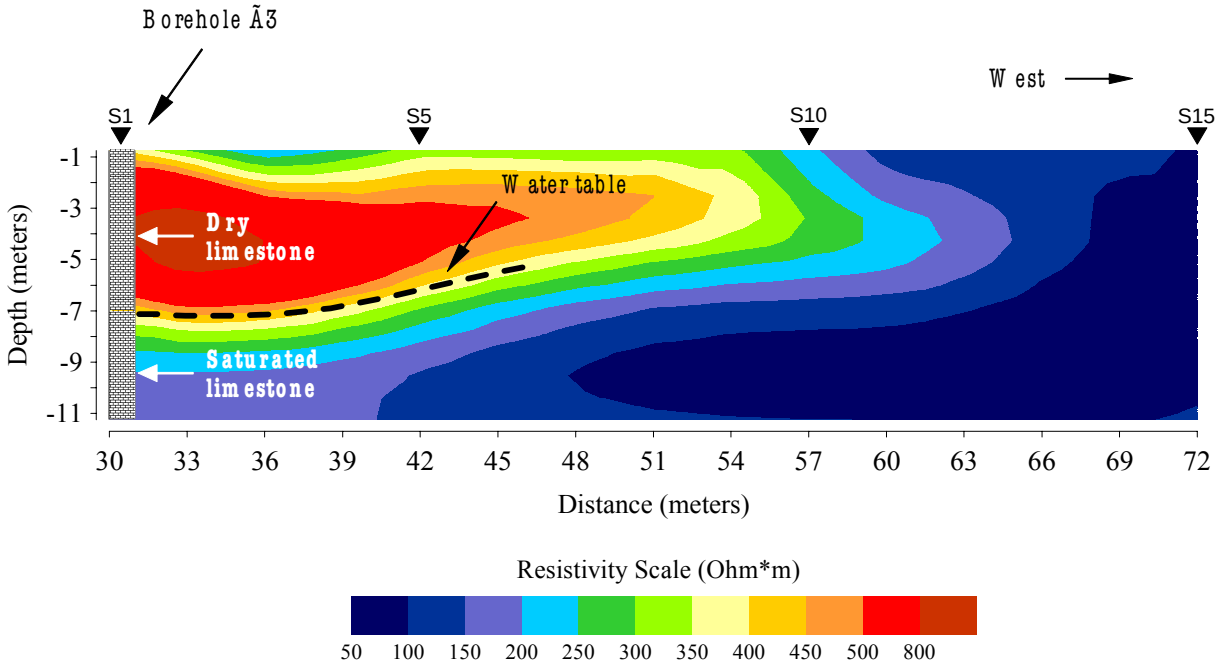

FIG. 12. Interpreted resistivity section for line LAKKA-3.

RESULTS AND INTERPRETATION

Line LAKKA-3

Resistivity tomography was conducted at the northwest end of Lakka mass along the main road north of Lakka carbonates (Fig. 1). It consists of fifteen DC resistivity soundings with station spacing of 3 m resulting in a 42 m long line. In fact, this experiment was carried out in order to calibrate the resistivity measurements using the borehole Γ3 located at the east end of the line. Strong lateral resistivity variation is observed on the resistivity section (Fig. 12). According to the nearby monitoring borehole Γ3, the water table is located at a

depth of 7 m. On the resistivity section the water table is indicated by the broken line, which separates a high resistivity top layer and a conductive one. The conductive layer (ρ<50 Ohm.m) present on the western portion of the resistivity section is interpreted as clayey formations possibly acting as an aquitard.

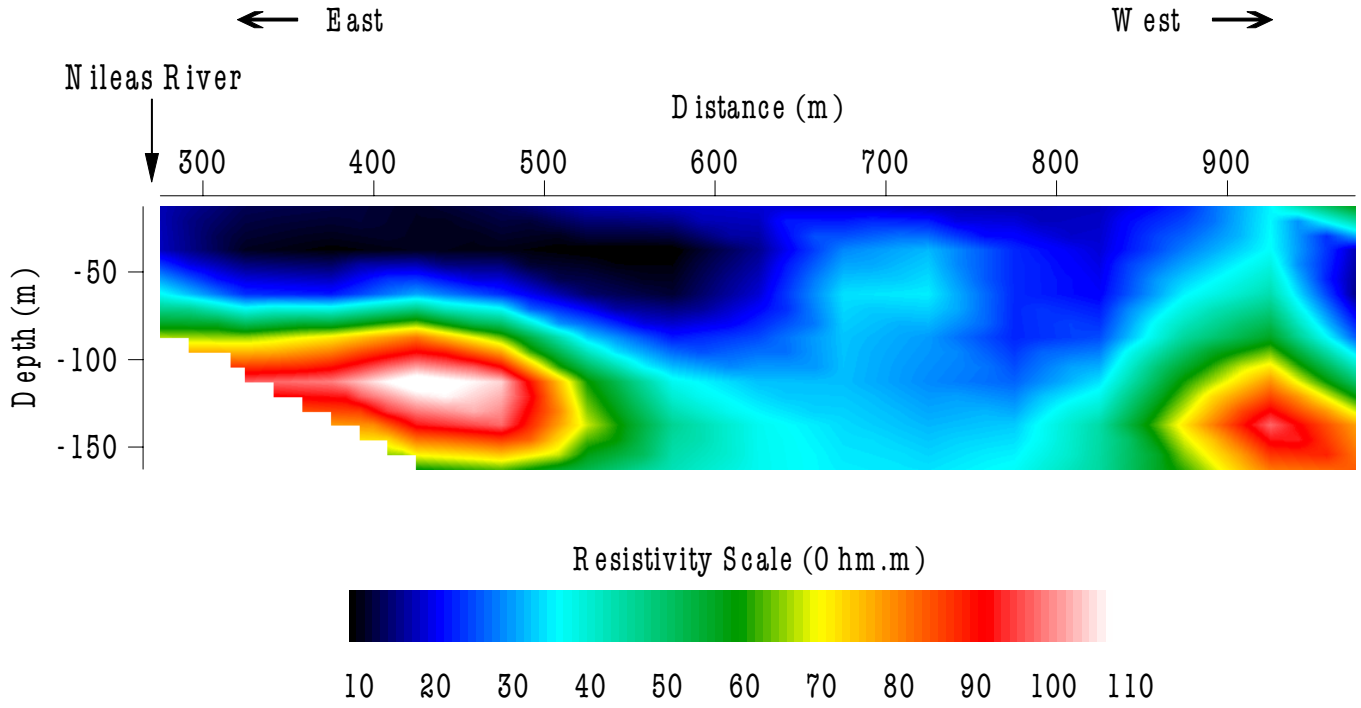

FIG. 13. Interpreted resistivity section for line LAKKA-5.

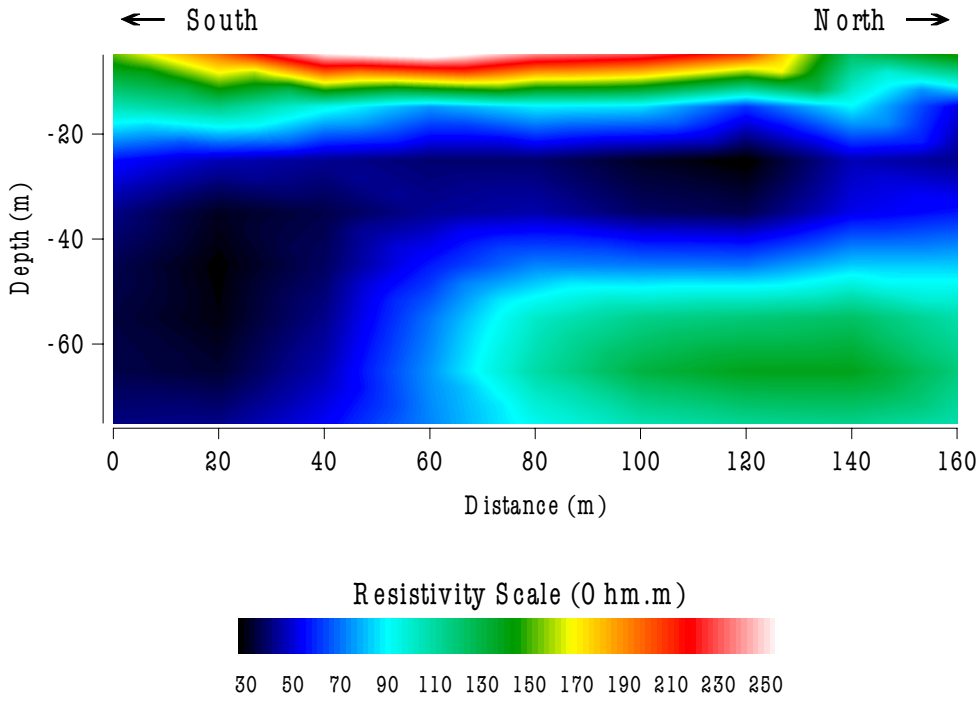

FIG. 14. Interpreted resistivity section for line LAKKA-6.

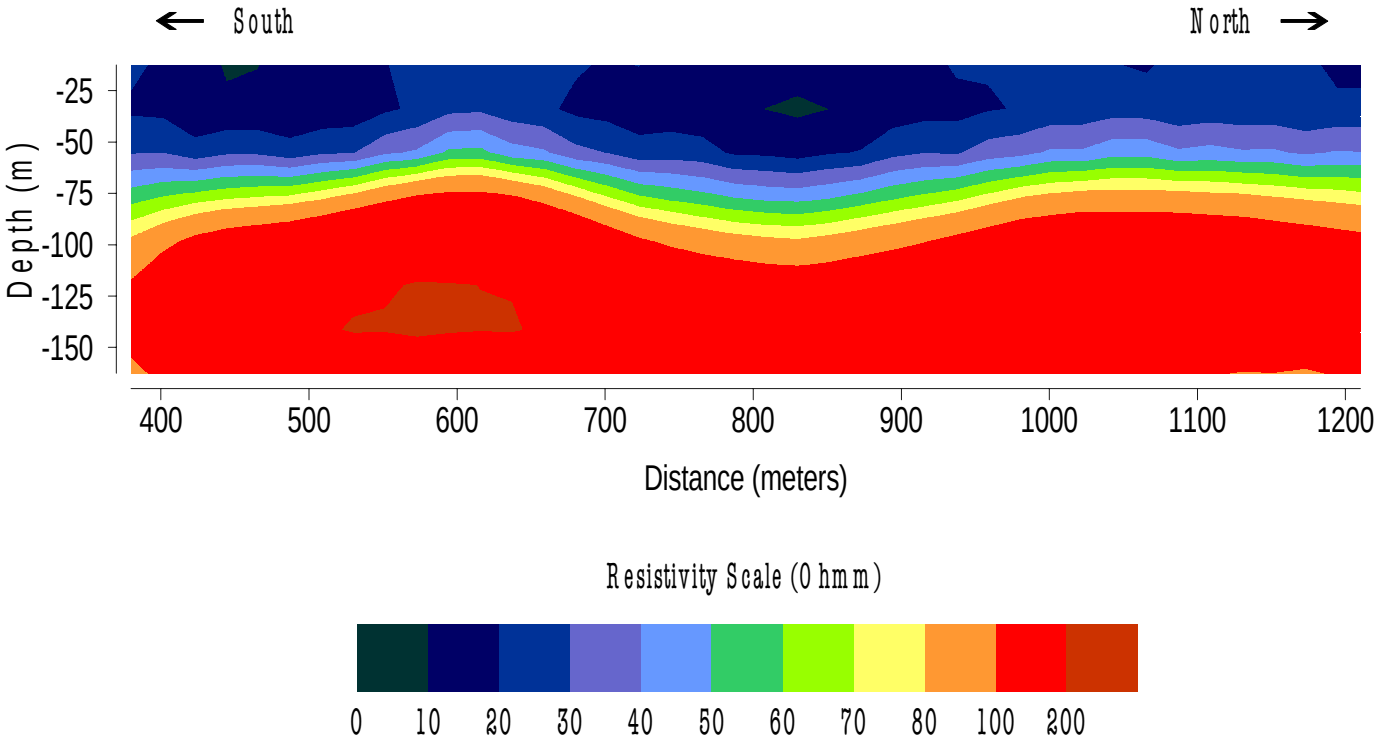

FIG. 15. Interpreted resistivity section for line LAKKA-4.

Line LAKKA-5

Line LAKKA-5 is located on the alluvial basin in the west of Lakka mass, (Fig. 1) along the main road connecting Mandoudi and Kirinthos villages. Fourteen DC resistivity soundings were conducted with station spacing of 50 m resulting in a profile of 650 m long. The resistivity section (Fig. 13) shows two layers, the top being conductive (ρ<40 Ohm.m) and the basement having intermediate resistivity values ranging between 80 and 130 Ohm.m.

The conductive layer is dipping to the west. Its thickness varies from about 60 m near the river to 100 m at the middle of the line. From the surface geology, the boreholes and insitu resistivity measurements of outcrops, this layer consists of clayey formations, which constitute the base of the river possibly acting as aquitard.

Line LAKKA-6

Line LAKKA-6 is parallel to the river on a narrow alluvial zone separating the exposures of Lakka mass (Fig. 1). Nine DC resistivity soundings were conducted with station spacing of 20 meters resulting in a 160 m long line. The resistivity section (Fig. 14) shows a top layer of intermediate resistivity (130 to 250 Ohm.m) and a mean thickness of 5 m. It is attributed to river sand and gravel.

A deeper conductive layer (ρ<60 Ohm.m) exhibits a constant thickness of about 30 m for distances ranging from 60 to 160 m and becomes very thick to the south. This conductive layer is also attributed to the presence of clayey formations acting as barrier between the river's waters and Lakka aquifer. This is additionally supported by the fact that no infiltration of waters from the river towards the system of Lakka carboniferous mass was observed during the pumping tests for boreholes Γ0 and Γ1.

Line LAKKA-4

Line LAKKA-4, located at the northern part of the area under investigation (Fig. 1), is parallel to the river. Eighteen DC resistivity soundings were conducted with station spacing of 50 m resulting in a 1200 m long line. The resistivity section (Fig. 15) also shows a shallow conductive layer (ρ<50 Ohm.m) on top of a resistive one. The thickness of the conductive layer varies from 60 m to about 100 m at the middle of the profile line.

CONCLUSION

Non-destructive geophysical techniques contributed to the understanding of Lakka karst aquifer. Complementary and compatible results have been derived from the application of seismic and electrical methods in Mandoudi.

The velocity variation for the very shallow subsurface is deduced from the seismic refraction depth section. Deeper interfaces are present on the stacked section. The water table and the base of the limestone are mapped by the combination of the results of seismic reflection and refraction methods. The water table is also present on the resistivity sections. The water table depth deduced from the geophysical survey is in agreement with the one measured in nearby boreholes. The active thickness of the karst aquifer was subsequently determined. Electrical tomography gave valuable information concerning the hydraulic communication between Lakka aquifer and Nileas River. The resulting geophysical models were useful for building conceptual geological/hydrogeological model of the aquifer, which is the basis for guiding the drilling program for the irrigation of the plain areas in the north and east of Mandoudi.

REFERENCES

Lekkas, S., and Alexopoulos, A., 1998. Hydrogeological study of Nileas and Kireas rivers basin: Technical Report, Dept. of Applied Geology, Univ. of Athens.

Louis, I., 1998. Geophysical investigations in Nileas River basin, Mandoudi, Euboea: Technical Report, Geophysics & Geothermics Dept., Univ. of Athens.

Palmer, D., 1981. An introduction to the generalized reciprocal method of seismic refraction interpretation: Geophysics, **46**, 1508-1518.

Telford, W. M., Geldart, L. P., and Sheriff, R. A., 1990. Applied Geophysics: 2nd edition, Cambridge Univ. Press.

Tsourlos, P., 1995. Modelling, interpretation and inversion of multi-electrode resistivity survey data: PhD Thesis, University of York.

Tsourlos, P., Szymanski, J., and Tsokas, G., 1998. A smoothness constrained algorithm for the fast 2D inversion of DC resistivity and induced polarization data: Journal of the Balkan Geophysical Society, **1**, 3-13.

Widess, W. B., 1973. How thin is a thin bed?: Geophysics, **38**, 1176-1180.